

QCD analysis of polarized DIS and the SIDIS asymmetry world data and light sea-quark decomposition

F. Arbabifar,^{*} Ali N. Khorramian,[†] and M. Soleymaninia[‡]

*Physics Department, Semnan University, Semnan, Iran
School of Particles and Accelerators, Institute for Research in
Fundamental Sciences (IPM), P.O.Box 19395-5531, Tehran, Iran
(Dated: October 9, 2018)*

The results of our new QCD analysis of helicity parton distributions of the nucleon at full next-to-leading order (NLO) accuracy in the fixed-flavor number scheme will be presented. Performing a combined QCD fit on the global sets of latest inclusive and the semi-inclusive polarized deep inelastic scattering data, we are able to extract new polarized parton distribution functions (PPDFs) at the input scale $Q_0^2 = 1 \text{ GeV}^2$. Particular, we have calculated PPDFs considering light sea-quark decomposition and the results are compared with the experimental data and the most precise theoretical models obtained by recent analyses. The latest COMPASS2010 SIDIS data, which were not available for the previous analyses, are employed in the current analysis and the effect of COMPASS SIDIS data is studied in detail. Also the uncertainties of PPDFs are determined using the standard Hessian technique.

PACS numbers: 13.60.Hb, 12.39.-x, 14.65.Bt

I. INTRODUCTION

In the recent years the determination of nucleon partonic composition and their spin projections from high energy experimental data has improved remarkably and the extracted polarized and unpolarized partonic distributions have very essential role in the study of hard scattering processes phenomenology. For the case of polarized parton distributions, the experimental discoveries of nucleon spin in the late 1980's [1, 2] proved the spin contribution of valence quarks is anomalously small and the predictions are far from reality, then the theoretical assumptions on perturbative QCD were applied to interpret theses experimental results [3–7].

In the recent decades the determination of PPDFs and their uncertainties from deep inelastic scattering (DIS) experiments performing at CERN, SLAC, DESY and JLAB [8–20] spread very fast [21–46] and recently semi inclusive deep inelastic scattering (SIDIS) experimental data [16, 47–49] have been also included by some of the theoretical groups [50–54]. The only theoretical group which perform a combined NLO analysis of DIS, SIDIS and polarized proton proton collision data was DSSV in 2008 [55]. The extracted PPDFs of valence quarks lightly differ but the PPDFs of sea quarks and gluon are more different caused by datasets selection, parametrization forms of PPDFs and the method of evolution and QCD analysis. The effect of different PPDFs and the spin Physics on the determination of fragmentation functions have been studied recently in Ref. [56]

In our latest analysis we studied the impact of inclusive

DIS data on the determination of PPDFs based on Jacobi polynomials with flavor symmetric light sea distribution, i.e. $\delta\bar{u} = \delta\bar{d} = \delta\bar{s} = \delta s$ [22], and now we consider light sea-quark decomposition and include additional SIDIS data [16, 47–49, 57]. In fact, fully inclusive DIS data from many different experiments are just impressive to determine the sum of the quark and anti-quark distributions while SIDIS data help to tell difference between quarks and anti-quarks as well. Here we focus on the effect of SIDIS data on determination of PPDFs, specially sea quarks distribution separation which was not considered in our last DIS data analysis and we present the comparison between both results. The impact of RHIC polarized proton proton collision data will be studied in a separate publication in near future.

In the present analysis we utilize the full sets of proton and deuteron SIDIS asymmetry data from the COMPASS group at CERN [48, 49, 57] which were partially considered by the last analysis on SIDIS data [50, 55]. Specially we use the new semi inclusive asymmetries COMPASS2010 proton data for charged pions and kaons production from polarized proton target, A_1^{p,π^\pm} and A_1^{p,k^\pm} [57], which were not available for the analysis before 2010 and are helpful to study δs and $\delta\bar{s}$ distributions due to kaon detection from polarized proton for the first time [57]. In order to discuss more about the effect of COMPASS SIDIS data on polarized \bar{u} , \bar{d} and $s = \bar{s}$ we perform extra analysis excluding these datasets. The comparison of results shows the effect of their inclusion clearly.

The current study presents a new NLO QCD analysis of the polarized DIS and SIDIS data and we extract new parametrization forms of PPDFs in flavor SU(2) and SU(3) symmetry breaking. Here we also propose a simplified form of double Mellin convolution expressions which saves times during fitting procedure. Also the behavior of $\Delta\chi^2$ and the uncertainty of PPDFs are calculated using

^{*}Electronic address: farbabifar@ipm.ir

[†]Electronic address: khorramiana@theory.ipm.ac.ir

[‡]Electronic address: maryam_soleimannia@ipm.ir

the standard Hessian method.

This paper is organized as follows. In Sec. II we present the relationship between polarized structure functions and asymmetry data as observables and then we review the datasets used in our analysis on PPDFs. QCD analysis including parametrization, evolution and simplification of double Mellin convolution of PPDFs, Wilson coefficients and FFs are discussed in Sec. III. Sec. IV presents the fitting procedure and global χ^2 minimization for asymmetry data and the investigation of χ^2 neighborhood and error calculation by standard Hessian method. We present the full results of our fit to the data, comparison with other models and sum rules in Sec. V and finally Sec. VI contains the summary of the whole work.

II. EXPERIMENTAL OBSERVABLES AND DATASETS

A. Polarized asymmetries

Perturbative QCD can predict polarized structure function $g_1(x, Q^2)$ in terms of PPDFs and strong coupling constant up to NLO approximation. However, experimental groups measure cross section asymmetries A_{\parallel} and A_{\perp} defined by the following ratios

$$\begin{aligned} A_{\parallel} &= \frac{d\sigma^{\rightarrow\rightarrow} - d\sigma^{\rightarrow\leftarrow}}{d\sigma^{\rightarrow\rightarrow} + d\sigma^{\rightarrow\leftarrow}}, \\ A_{\perp} &= \frac{d\sigma^{\rightarrow\uparrow} - d\sigma^{\rightarrow\downarrow}}{d\sigma^{\rightarrow\uparrow} + d\sigma^{\rightarrow\downarrow}}, \end{aligned} \quad (1)$$

where $d\sigma^{\rightarrow\rightarrow}$ and $d\sigma^{\rightarrow\leftarrow}$ are cross sections for longitudinal polarized lepton scattering of a parallel or anti-parallel polarized target hadron, and $d\sigma^{\rightarrow\uparrow}$ and $d\sigma^{\rightarrow\downarrow}$ are the same for a transversely polarized hadron.

The ratio of polarized and unpolarized structure functions, g_1 and F_1 , is related to the measurable asymmetries by

$$\frac{g_1(x, Q^2)}{F_1(x, Q^2)} = \frac{1}{(1 + \gamma^2)(1 + \eta\zeta)} \left[(1 + \gamma\zeta) \frac{A_{\parallel}}{D} - (\eta - \gamma) \frac{A_{\perp}}{d} \right], \quad (2)$$

and the definitions of kinematic factors are given by

$$\gamma = \frac{2Mx}{\sqrt{Q^2}}, \quad (3)$$

$$d = \frac{D\sqrt{1 - y - \gamma^2 y^2/4}}{1 - y/2}, \quad (4)$$

$$D = \frac{1 - (1 - y)\epsilon}{1 + \epsilon R(x, Q^2)}, \quad (5)$$

$$\eta = \frac{\epsilon\gamma y}{1 - \epsilon(1 - y)}, \quad (6)$$

$$\zeta = \frac{\gamma(1 - y/2)}{1 + \gamma^2 y/2}, \quad (7)$$

$$\epsilon = \frac{4(1 - y) - \gamma^2 y^2}{2y^2 + 4(1 - y) + \gamma^2 y^2}, \quad (8)$$

here M denotes the nucleon mass and $y = (E - E')/E$ describes the normalized energy fraction transferred to the virtual photon, with E the energy of incoming lepton and E' the energy of scattered lepton in the nucleon rest frame. The unpolarized structure function F_1 is expressed by its expression in terms of measured unpolarized structure function F_2 extracted from unpolarized DIS experiments [58]

$$F_1(x, Q^2) = \frac{(1 + \gamma^2)}{2x(1 + R(x, Q^2))} F_2(x, Q^2), \quad (9)$$

and R is the ratio of longitudinal to transverse photon-nucleon unpolarized structure function which is determined in Ref. [59]

$$R(x, Q^2) = \frac{F_L(x, Q^2)}{F_2(x, Q^2) - F_L(x, Q^2)}. \quad (10)$$

The asymmetries A_{\parallel} and A_{\perp} can be expressed in terms of A_1 and A_2 , which are the virtual-photon longitudinal and transverse asymmetries, by

$$\begin{aligned} A_{\parallel} &= D(A_1 + \eta A_2), \\ A_{\perp} &= d(A_2 - \zeta A_1), \end{aligned} \quad (11)$$

where

$$\begin{aligned} A_1(x, Q^2) &= \frac{\sigma_{1/2}^T - \sigma_{3/2}^T}{\sigma_{1/2}^T + \sigma_{3/2}^T}, \\ A_2(x, Q^2) &= \frac{2\sigma^{TL}}{\sigma_{1/2}^T + \sigma_{3/2}^T}. \end{aligned} \quad (12)$$

Note that $\sigma_{1/2}^T$ and $\sigma_{3/2}^T$ recall the virtual transversely polarized photon scattering cross sections when the total spin of photon-nucleon system is 1/2 or 3/2 respectively, and σ^{TL} is the term denoting the interference of longitudinal and transverse photon-nucleon amplitudes. Finally using Eqs. 11 and 2 one can find the relation between polarized and unpolarized structure functions g_1 and F_1 , and the asymmetries A_1 and A_2 [60]

$$\frac{g_1}{F_1} = \frac{1}{1 + \gamma^2} [A_1 + \gamma A_2]. \quad (13)$$

The value of A_2 has been determined by SMC [61], E154 [62] and E143 [63] and the measurements showed its contribution to g_1/F_1 can be neglected in a good approximation, also it is being suppressed by the small value of kinematic factor γ in the limit $m^2 \ll Q^2$.

In our QCD analysis we perform fit procedure on A_1 or g_1/F_1 for DIS data

$$A_1(x, Q^2) = \frac{g_1(x, Q^2)}{F_1(x, Q^2)} (1 + \gamma^2). \quad (14)$$

Note that such a procedure is equivalent to a fit to $(g_1)_{exp}$, but it is more precise than the fit to the g_1 data themselves presented by the experimental groups because

here the g_1 data are extracted in the same way for all of the datasets.

Unlike the inclusive polarized deep inelastic scattering wherein g_1 structure function is measured by detecting only the final state lepton, the particle detected in semi inclusive polarized deep inelastic experiments are charged hadrons in addition to scattered lepton. When the energy fraction of hadron, $z = E_h/E_\gamma$ is large, the most possible occurrence of detected hadrons are π^\pm and k^\pm which include struck quarks in their valance state. The double-spin asymmetry in SIDIS experiments for the production of hadron h is

$$A_{1N}^h(x, z, Q^2) = \frac{g_{1N}^h(x, z, Q^2)}{F_{1N}^h(x, z, Q^2)}. \quad (15)$$

The structure functions g_1^h and F_1^h are fully determined in terms of polarized and unpolarized distributions respectively up to NLO approximation and will be discussed in Sec III. Thus we will determine g_1 and g_{1N}^h from Eqs. 14 and 15 in the analysis and extract polarized parton distribution functions.

B. The datasets and ranges

We utilize two types of datasets from DIS and SIDIS experiments which come from relevant experiments done at DESY, SLAC, JLAB and CERN. The datasets used in our QCD analysis are summarized in Table I. These experiments have different targets, including protons, neutrons and deuterons, and also different detected hadrons, including π^\pm , k^\pm and h^\pm , for SIDIS reactions. We also show the number of data and the kinematic cuts on the experiments in Table I, we exclude the data points which are in the range of $Q^2 < 1$ from our analysis, since below $Q^2 = 1$ GeV² perturbative QCD is not reliable. The summary of observables is as follows:

- **EMCp, SMCpd, COMPASS, E142, E143, E154, E155 HERMES and JLAB DIS data**

These experiments all determined A_1 except of E155 [14, 15] and HERMES [17] which present g_1/F_1 and JLAB [19] present both measurements. Since we consider different masses of nucleons in γ in Eq. 14, we distinguish these two data types.

- **SMCpd, HERMES and COMPASS SIDIS data**

These experiments measure A_{1N}^h as in Eq. 15 from semi inclusive reactions. The very recent and precise proton data of COMPASS [57] are used for the first time in the current analysis. Figs 1 and 2 shows the DIS and SIDIS used data points in a scatter plot, as can be seen the region of x and Q^2 is restricted to $0.004 \lesssim x \lesssim 0.75$ and $1.0 \lesssim Q^2 \lesssim 60$ GeV² for DIS and $0.005 \lesssim x \lesssim 0.5$ and $1.0 \lesssim Q^2 \lesssim 60$ GeV² for SIDIS experiments. We try to use all available data for DIS and SIDIS experiments to cover a large range of kinematics variables in comparison to other recent analysis [24, 50, 55].

III. DETERMINATION OF POLARIZED PDFS FROM OBSERVABLES

A. Theoretical framework

The idea behind our present analysis is to extract the universal polarized PDFs entering factorized cross sections by optimizing the agreement between the measured asymmetries from DIS and SIDIS experiments, relative to the accuracy of the data, and corresponding theoretical calculations, through variation of the shapes of the polarized PDFs. Considering perturbative QCD, the structure function $g_1(x, Q^2)$ can be written in NLO approximation as a Mellin convolution of the PPDFs, including gluon, with the corresponding Wilson coefficient functions $\delta C_{q,g}$ [6] by

$$g_1(x, Q^2) = \frac{1}{2} \sum_{q, \bar{q}}^{n_f} e_q^2 \left\{ \left[1 + \frac{\alpha_s}{2\pi} \delta C_q \right] \otimes \delta q(x, Q^2) + \frac{\alpha_s}{2\pi} 2\delta C_g \otimes \delta g(x, Q^2) \right\}, \quad (16)$$

here e_q denotes the charge of the quark flavor and $\{\delta q, \delta \bar{q}, \delta g\}$ are the polarized quark, anti-quark, and gluon distributions, respectively.

For the SIDIS asymmetry of Eq. 15 we have the following forms for polarized and unpolarized structure functions in NLO approximation

$$g_{1N}^h(x, z, Q^2) = \frac{1}{2} \sum_{q, \bar{q}}^{n_f} e_q^2 \left\{ \left[\delta q \left(1 + \otimes \frac{\alpha_s(Q^2)}{2\pi} \delta C_{qq} \right) D_q^h + \delta q \otimes \frac{\alpha_s(Q^2)}{2\pi} \delta C_{gq}^{(1)} \otimes D_g^h + \delta g \otimes \frac{\alpha_s(Q^2)}{2\pi} \delta C_{gg}^{(1)} \otimes D_g^h \right] (x, z, Q^2) \right\}, \quad (17)$$

and

$$F_{1N}^h(x, z, Q^2) = \frac{1}{2} \sum_{q, \bar{q}}^{n_f} e_q^2 \left\{ \left[q \left(1 + \otimes \frac{\alpha_s(Q^2)}{2\pi} C_{qq} \right) D_q^h + q \otimes \frac{\alpha_s(Q^2)}{2\pi} C_{gq}^{(1)} \otimes D_g^h + g \otimes \frac{\alpha_s(Q^2)}{2\pi} C_{gg}^{(1)} \otimes D_g^h \right] (x, z, Q^2) \right\}, \quad (18)$$

where δq and q denote polarized and unpolarized parton distributions, $\delta C_{ij}^{(1)}(x, z)$ and $C_{ij}^{(1)}(x, z)$, $i, j = q, g$, are Wilson coefficient functions presented in Ref. [64] in the $\overline{\text{MS}}$ scheme. Also $D_{q, \bar{q}}^h$, D_g^h denote the corresponding fragmentation functions and n_f presents the number

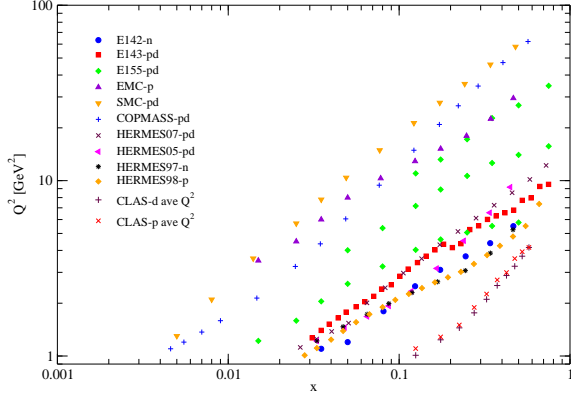
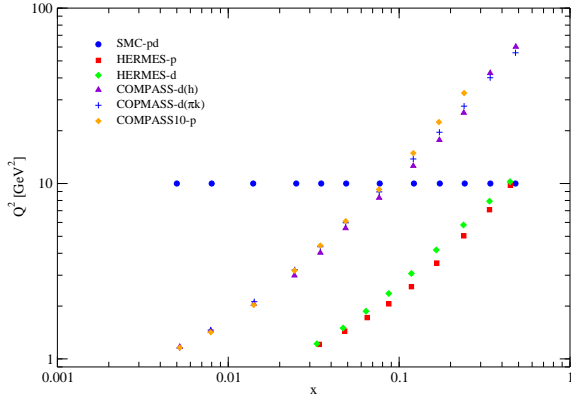
Experiment	Process	N_{data}	x_{min}	x_{max}	Q_{min}^2 [GeV ²]	Q_{max}^2 [GeV ²]	F	χ^2
EMC [8]	DIS(p)	10	0.015	0.466	3.5	29.5	A_1^p	3.9
SMC [9]	DIS(p)	12	0.005	0.48	1.3	58	A_1^p	3.4
SMC [9]	DIS(d)	12	0.005	0.479	1.3	54.8	A_1^d	17.1
COMPASS [10]	DIS(p)	15	0.0046	0.568	1.1	62.1	A_1^p	20.5
COMPASS [10]	DIS(d)	15	0.0046	0.566	1.1	55.3	A_1^d	13.6
SLAC/E142 [11]	DIS(n)	8	0.035	0.466	1.1	5.5	A_1^n	4.18
SLAC/E143 [12]	DIS(p)	28	0.031	0.749	1.27	9.52	A_1^p	22.0
SLAC/E143 [12]	DIS(d)	28	0.031	0.749	1.27	9.52	A_1^d	54.6
SLAC/E154 [13]	DIS(n)	11	0.017	0.564	1.2	15	A_1^n	3.3
SLAC/E155 [14]	DIS(p)	24	0.015	0.75	1.22	34.72	$\frac{g_1^p}{F_1^p}$	22.5
SLAC/E155 [15]	DIS(d)	24	0.015	0.75	1.22	34.72	$\frac{g_1^d}{F_1^d}$	21.4
HERMES [16]	DIS(p)	9	0.033	0.447	1.22	9.18	A_1^p	4.5
HERMES [16]	DIS(d)	9	0.033	0.447	1.22	9.16	A_1^d	11.4
HERMES [17]	DIS(n)	9	0.033	0.464	1.22	5.25	A_1^n	2.5
HERMES [17]	DIS(p)	19	0.028	0.66	1.01	7.36	$\frac{g_1^p}{F_1^p}$	21.4
HERMES [18]	DIS(p)	15	0.0264	0.7248	1.12	12.21	A_1^p	10.2
HERMES [18]	DIS(d)	15	0.0264	0.7248	1.12	12.21	A_1^d	16.7
JLab-Hall A [19]	DIS(n)	3	0.33	0.6	2.71	4.38	$\frac{g_1^n}{F_1^n}$	0.8
CLAS [20]	DIS(p)	151	0.1088	0.5916	1.01	4.96	A_1^p	151.0
CLAS [20]	DIS(d)	482	0.1366	0.57	1.01	4.16	A_1^d	442.5
SMC [47]	SIDIS(p, h^+)	12	0.005	0.48	10	10	A_1^{p,h^+}	23.0
SMC [47]	SIDIS(p, h^-)	12	0.005	0.48	10	10	A_1^{p,h^-}	11.9
SMC [47]	SIDIS(d, h^+)	12	0.005	0.48	10	10	A_1^{d,h^+}	6.3
SMC [47]	SIDIS(d, h^-)	12	0.005	0.48	10	10	A_1^{d,h^-}	17.2
HERMES [16]	SIDIS(p, h^+)	9	0.034	0.448	1.21	9.76	A_1^{p,h^+}	15.0
HERMES [16]	SIDIS(p, h^-)	9	0.034	0.448	1.21	9.76	A_1^{p,h^-}	6.0
HERMES [16]	SIDIS(d, h^+)	9	0.033	0.446	1.21	9.61	A_1^{d,h^+}	10.3
HERMES [16]	SIDIS(d, h^-)	9	0.033	0.446	1.21	9.61	A_1^{d,h^-}	8.9
HERMES [16]	SIDIS(p, π^+)	9	0.033	0.449	1.22	10.46	A_1^{p,π^+}	9.7
HERMES [16]	SIDIS(p, π^-)	9	0.033	0.449	1.22	10.46	A_1^{p,π^-}	7.7
HERMES [16]	SIDIS(d, π^+)	9	0.033	0.446	1.22	10.24	A_1^{d,π^+}	18.2
HERMES [16]	SIDIS(d, π^-)	9	0.033	0.446	1.22	10.24	A_1^{d,π^-}	25.0
HERMES [16]	SIDIS(d, k^+)	9	0.033	0.447	1.22	10.26	A_1^{d,k^+}	10.3
HERMES [16]	SIDIS(d, k^-)	9	0.033	0.447	1.22	10.26	A_1^{d,k^-}	6.1
COMPASS [48]	SIDIS(d, h^+)	12	0.0052	0.482	1.17	60.2	$A_d^{h^+}$	18.1
COMPASS [48]	SIDIS(d, h^-)	12	0.0052	0.482	1.17	60.2	$A_d^{h^-}$	20.2
COMPASS [49]	SIDIS(d, π^+)	10	0.0052	0.24	1.16	32.8	$A_d^{\pi^+}$	13.8
COMPASS [49]	SIDIS(d, π^-)	10	0.0052	0.24	1.16	32.8	$A_d^{\pi^-}$	14.6
COMPASS [49]	SIDIS(d, k^+)	10	0.0052	0.24	1.16	32.8	$A_d^{k^+}$	24.0
COMPASS [49]	SIDIS(d, k^-)	10	0.0052	0.24	1.16	32.8	$A_d^{k^-}$	14.4
COMPASS10 [57]	SIDIS(p, π^+)	12	0.0052	0.48	1.16	55.6	$A_p^{\pi^+}$	15.7
COMPASS10 [57]	SIDIS(p, π^-)	12	0.0052	0.48	1.16	55.6	$A_p^{\pi^-}$	11.2
COMPASS10 [57]	SIDIS(p, k^+)	12	0.0052	0.48	1.16	55.6	$A_p^{k^+}$	14.3
COMPASS10 [57]	SIDIS(p, k^-)	12	0.0052	0.48	1.16	55.6	$A_p^{k^-}$	6.4
TOTAL:		1149						1171.5

TABLE I: Published data points from experimental groups, the process which they are extracted from, the number of them (with a cut of $Q^2 \geq 1.0$ GeV²), their kinematic range, the measured observables and the χ^2 values for each set.

of active flavors which we take $n_f = 3$ in the present analysis.

As can be seen, the SIDIS asymmetries depend on the hadronic variable $z = p_h \cdot p_N / p_N \cdot q$ in addition to x and Q^2 . Here z denotes the momentum fractions taking by the resulting hadron from the scattered parton and p_h , p_N and q are the usual hadron, nucleon and photon four

momentum, respectively. Since experimental collaborations do not present the z variable of presented SIDIS data points, we integrate over $z > 0.2$, which comes from the current fragmentation functions region, for both $g_1(x, z, Q^2)$ and $F_1(x, z, Q^2)$ to cancel the z dependance

FIG. 1: DIS used data in a (x, Q^2) plane.FIG. 2: SIDIS used data in a (x, Q^2) plane.

of A_{1N}^h [65]

$$A_{1N}^h(x, z, Q^2) = \frac{\int_{0.2}^1 dz g_{1N}^h(x, z, Q^2)}{\int_{0.2}^1 dz F_{1N}^h(x, z, Q^2)}. \quad (19)$$

One of the most important ingredient of SIDIS data analysis is the choice of fragmentation functions [66]. Although there are different available analysis of FFs [56, 67, 68], here we use the latest DSS [69] NLO FFs and for unpolarized PDFs we choose MRST02 [70] parametrization like DSSV09 and LSS10 [50, 55] to make our analysis comparable with them. Also, in addition to the precision of above FFs and PDFs and comparability, we use them together since DSS FFs were extracted from SIDIS data using MRST02 unpolarized PDFs.

Considering isospin symmetry, one can relate proton and neutron parton distributions

$$\begin{aligned} \delta u^p &= \delta d^n, \quad \delta \bar{u}^p = \delta \bar{d}^n, \\ \delta d^p &= \delta u^n, \quad \delta \bar{d}^p = \delta \bar{u}^n, \\ \delta s^p &= \delta s^n, \quad \delta \bar{s}^p = \delta \bar{s}^n, \end{aligned} \quad (20)$$

so the polarized structure function of neutron g_1^n can be obtained from all of Eqs. 16, 17 and 18 by just replacing

up quarks PPDFs and FFs by down ones. Also deuteron structure functions are given in terms of proton and neutron ones

$$g_{1d}^{(h)} = \frac{1}{2}(g_{1p}^{(h)} + g_{1n}^{(h)})(1 - 1.5 \omega_D), \quad (21)$$

where $\omega_D = 0.05$ is the probability to find the deuteron in a D state. Now by having PPDFs and all other ingredients, we are able to make polarized asymmetry function from DIS and SIDIS precesses.

B. PPDFs Parametrization

In our analysis we choose an initial scale for the evolution of $Q_0^2 = 1 \text{ GeV}^2$ and assume the PPDFs to have the following functional form

$$x \delta q = \mathcal{N}_q \eta_q x^{a_q} (1-x)^{b_q} (1 + c_q x^{0.5} + d_q x), \quad (22)$$

with $\delta q = \delta u + \delta \bar{u}$, $\delta d + \delta \bar{d}$, $\delta \bar{u}$, $\delta \bar{d}$, $\delta \bar{s}$ and δg . The Normalization constants \mathcal{N}_q

$$\begin{aligned} \frac{1}{\mathcal{N}_q} &= \left(1 + d_q \frac{a_q}{a_q + b_q + 1} \right) B(a_q, b_q + 1) \\ &+ c_q B\left(a_q + \frac{1}{2}, b_q + 1\right), \end{aligned} \quad (23)$$

are chosen such that η_q are the first moments of $\delta q(x, Q_0^2)$ and $B(a, b)$ is the Euler beta function. Since the present SIDIS data are not yet sufficient to distinguish s from \bar{s} , we assume $\delta s(x, Q^2) = \delta \bar{s}(x, Q^2)$ throughout.

To control the behavior of PPDFs, we have to consider some extra constraints; so we get $a_{u+\bar{u}} = a_{\bar{u}}$ and $a_{d+\bar{d}} = a_{\bar{d}} = a_s$ to control the small x behavior of \bar{u} , \bar{d} and $s = \bar{s}$. Also in the primary fitting procedures we find out that the parameters $b_{\bar{u}}$, $b_{\bar{d}}$, $b_{s=\bar{s}}$ and b_g become very close to each other, around 10. We understand that they are not strongly determined by the fit, so we fix them to 10 which is their preferred value to fulfill the positivity condition, $|\delta q_i(x, Q_0^2)| \leq q_i(x, Q_0^2)$ [71], and also it controls the behavior of polarized sea quarks at large x region. In addition, we find that the parameter c_q is very close to zero for $\delta q = \delta u + \delta \bar{u}$, $\delta d + \delta \bar{d}$, $\delta \bar{s}$ and δg so we fix them at 0.

Generally PPDFs analyses use two well-known sum rules relating the first moments of PPDFs to F and D quantities which are evaluated in neutron and hyperon β -decays [72] under the assumption of SU(2) and SU(3) flavor symmetries

$$a_3 = \Delta \Sigma_u - \Delta \Sigma_d = F + D, \quad (24)$$

$$a_8 = \Delta \Sigma_u + \Delta \Sigma_d - 2 \Delta \Sigma_s = 3F - D, \quad (25)$$

where a_3 and a_8 denote non-singlet combinations of the first moments of the polarized parton distributions corresponding to non-singlet q_3 and q_8 distributions

$$q_3 = (\delta u + \delta \bar{u}) - (\delta d + \delta \bar{d}), \quad (26)$$

$$q_8 = (\delta u + \delta \bar{u}) + (\delta d + \delta \bar{d}) - 2(\delta s + \delta \bar{s}). \quad (27)$$

A new reanalysis of F and D parameters with updated β -decay constants acquired [72] $F = 0.464 \pm 0.008$ and $D = 0.806 \pm 0.008$, so we make use of these evaluations in our present analysis; however, since we do not focus on flavor symmetry and we have $\delta\bar{u} \neq \delta\bar{d} \neq \delta s$, we can use the combination of Eqs. 24 and 25 as following

$$\begin{aligned}\Delta u + \Delta\bar{u} &= 0.9275 + \Delta s + \Delta\bar{s} , \\ \Delta d + \Delta\bar{d} &= -0.3415 + \Delta s + \Delta\bar{s} ,\end{aligned}\quad (28)$$

and we apply the above relations in the analysis, so we exclude the parameters define the first moment of $(\delta u + \delta\bar{u})$ and $(\delta d + \delta\bar{d})$ (i.e. $\eta_{u+\bar{u}}$ and $\eta_{d+\bar{d}}$) from the analysis and obtain them by Eq. 28. The effect of symmetry breaking on the first moment of PPDFs have been discussed in detail in the literatures [55, 73].

C. Evolution & Computational method

For numerical calculations we need the scale evolution of the PPDFs from input scale Q_0^2 to each of the scales related to the data points. This evolution is done by a well-known set of integro-differential equations [74, 75] that can be easily solved analytically after a transformation from x space to Mellin N -moment space. The Mellin transform of a generic function f depending on momentum fraction x is defined as

$$f(N) \equiv \int_0^1 x^{N-1} f(x) dx . \quad (29)$$

The transformation (29) has the pleasant applied property that convolutions change to ordinary products, which veritabily simplifies calculations based on Mellin moments

$$[f \otimes g](N) \equiv \int_0^1 dx x^{N-1} \int_z^1 \frac{dy}{y} f\left(\frac{x}{y}\right) g(y) = f(N)g(N) , \quad (30)$$

it can be performed analytically not only for the relevant splitting functions governing the evolution of the PDFs but even for the partonic cross sections for both DIS and semi-inclusive DIS. The Mellin transform of the parton distributions q is defined similar to Eq. 29:

$$\begin{aligned}\delta q(N, Q_0^2) &= \int_0^1 x^{N-1} \delta q(x, Q_0^2) dx \\ &= \eta_q \mathcal{N}_q \left(1 + d_q \frac{N-1+a_q}{N+a_q+b_q} \right) \\ &\quad \times B(N-1+a_q, b_q+1) \\ &\quad + c_q B\left(N+a_q-\frac{1}{2}, b_q+1\right) ,\end{aligned}\quad (31)$$

where $q = \{u+\bar{u}, d+\bar{d}, \bar{u}, \bar{d}, s, g\}$ and B denotes the Euler beta function.

The inverse Mellin transform reads

$$f(x) \equiv \frac{1}{2\pi i} \int_{C_N} x^{-N} f(N) dN , \quad (32)$$

note that C_N is an appropriate contour in the complex N plane which has an imaginary part with the range from $-\infty$ to $+\infty$ and that crosses the real axis to the right of the rightmost pole of $f(N)$ [35].

Currently, in the case of using asymmetry data of SIDIS [50, 55] which depends on two scaling variables x and z according to Eqs. 17 and 18, Mellin transformation and the inverse of that requires straight extensions of Eqs. 29 and 32 to double transformations as was presented in Refs. [51, 76, 77].

Now for simplification of the double convolution in Eq. 17 we apply a method to change it to a single routine convolution by transforming the coefficients $\delta C_{ij}(x, z)$ from $x-z$ space to $N-z$ space

$$\int_0^1 x^{N-1} \delta C_{ij}(x, z) dx = \delta C_{ij}(N, z) , \quad (33)$$

and then we compute

$$\int_{0.2}^1 \delta C_{ij}(N, z) \otimes D_{i(j)}(z) = \delta \tilde{C}_{ij}(N) . \quad (34)$$

Finally we could have the evolution of NLO correction terms of g_{1N}^h in N -moment space according to Eqs. 17 and 30

$$\begin{aligned}g_{1N}^h(N) &= \frac{1}{2} \sum_{q, \bar{q}} e_q^2 \left\{ \int_{0.2}^1 dz \delta q D_q^h + \frac{\alpha_s(Q^2)}{2\pi} \delta q(N) \delta \tilde{C}_{qq}(N) \right. \\ &\quad + \frac{\alpha_s(Q^2)}{2\pi} \delta q(N) \delta \tilde{C}_{gq}(N) \\ &\quad \left. + \frac{\alpha_s(Q^2)}{2\pi} \delta g(N) \delta \tilde{C}_{qg}(N) \right\} ,\end{aligned}\quad (35)$$

the process is the same for Eq. 18. We calculate the transformation of Eq. 33 for all $C_{ij}(x, z)$ and $\delta C_{ij}(x, z)$ and provide them in Appendix.

IV. DETERMINATION OF MINIMUM χ^2 AND ERRORS

A. Minimization of χ^2

The process of global QCD analysis is based on the minimization of effective χ^2 which shows the quality of the fit carried out on datasets by variation of the input set of parameters. We use the QCD-PEGASUS program [78] for the evolution of distributions in N -moment space and the MINUIT package [79] for the minimization of χ^2 function

$$\chi^2 = \sum_i \left(\frac{A_{1,i}^{exp} - A_{1,i}^{theor}}{\Delta A_{1,i}^{exp}} \right)^2 , \quad (36)$$

here $A_{1,i}^{exp}$, $\Delta A_{1,i}^{exp}$, and $A_{1,i}^{theor}$ are the experimental measured value, the experimental uncertainty and theoretical value for the i^{th} data point, respectively. For the experimental error calculation the statistical and systematic errors of each data point are added in quadrature. Currently present available SIDIS data are not enough precise to determine strong coupling constant at input scale, so according to the precise scale dependent equation of $a_s = \frac{\alpha_s}{4\pi}$ used in PEGASUS in NLO [78]

$$\frac{1}{a_s(Q^2)} = \frac{1}{a_s(Q_0^2)} + \beta_0 \ln \left(\frac{Q^2}{Q_0^2} \right) - b_1 \ln \left\{ \frac{a_s(Q^2)[1 + b_1 a_s(Q_0^2)]}{a_s(Q_0^2)[1 + b_1 a_s(Q^2)]} \right\}, \quad (37)$$

we fixed $\alpha_s(Q_0^2) = 0.580$ which is corresponding to $\alpha_s(M_Z^2) = 0.119$, obtained from MRST02 analysis [70]. In Eq. 37 we have

$$\begin{aligned} \beta_0 &= 11 - \frac{2}{3}n_f, \\ \beta_1 &= 102 - \frac{38}{3}n_f, \\ b_1 &= \frac{\beta_1}{\beta_0}. \end{aligned} \quad (38)$$

Finally we minimize the χ^2 with the 17 unknown parameters. We work at NLO in the fixed-flavor number scheme $n_f = 3$ in the QCD evolution with massless partonic flavors.

B. The neighborhood of χ_0^2 and error determination via Hessian method

Here we just present the essential points for studying the neighborhood of χ_0^2 and the full procedure is provided in Refs. [70, 80, 81]. As mentioned in Sec. IV we find the appropriate parameter set which minimize the global χ^2 function, we call this PDF set S_0 and the parameters value of S_0 , i.e. $p_1^0 \dots p_n^0$, will be presented in Sec. V.

By moving away the parameters from their obtained values, χ^2 increases by the amount of $\Delta\chi^2$

$$\Delta\chi^2 = \chi^2 - \chi_0^2 = \sum_{i,j=1}^d H_{ij}(p_i - p_i^0)(p_j - p_j^0), \quad (39)$$

where the Hessian matrix H_{ij} is defined by

$$H_{ij} = \frac{1}{2} \frac{\partial^2 \chi^2}{\partial p_i \partial p_j} \Big|_{min}, \quad (40)$$

and we note $C \equiv H^{-1}$. Now it is convenient to work in term of eigenvalues and orthogonal eigenvectors of covariance matrix

$$\sum_{j=1}^n C_{ij} v_{jk} = \lambda_k v_{ik}, \quad (41)$$

also the displacement of parameter p_i from its minimum p_i^0 can be expressed in terms of rescaled eigenvectors $e_{ik} = \sqrt{\lambda_k} v_{ik}$

$$p_i - p_i^0 = \sum_{k=1}^n e_{ik} z_k, \quad (42)$$

putting Eq. 42 in 39 and considering the orthogonality of v_{ik} we have

$$\Delta\chi^2 = \sum_{k=1}^n z_k^2. \quad (43)$$

Now the relevant neighborhood of χ^2 is the interior of hypersphere with radius T :

$$\sum_{k=1}^n z_k^2 \leq T^2, \quad (44)$$

and the neighborhood parameters are given by

$$p_i(s_k^\pm) = p_i^0 \pm t e_{ik}, \quad (45)$$

with s_k is the k^{th} set of PDF and t adapted to make the desired $T = (\Delta\chi^2)^{\frac{1}{2}}$ and $t = T$ in the quadratic approximation. In Sec. V we present the dependance of $\Delta\chi^2$ along some random samples of eigenvector directions to test the quadratic approximation of Eq. 39.

Now we accompany the construction of the QCD fit by reliable estimation of uncertainty. As discussed in Refs. [70, 80, 81], the master equation to obtain the uncertainties of observables in modified Hessian method is

$$\Delta F = \frac{1}{2} \left[\sum_{k=1}^n (F(s_k^+) - F(s_k^-))^2 \right]^{\frac{1}{2}}, \quad (46)$$

here $F(s_k^+)$ and $F(s_k^-)$ are the value of F extracted from the input set of parameters $p_i(s_k^\pm)$ instead of p_i^0 mentioned in Eq. 45. However, it has been pointed out by DSSV [55] that the modified Hessian method is known to work reasonably well in extractions of spin independent parton densities and it is found to fail in the case of helicity parton densities for tolerances larger than $\Delta\chi^2 = 1$. So we prefer to calculate the PPDFs error band using standard Hessian method which is more reliable in this case. As presented in Eqs. 31 and 35, the evolved polarized parton densities and structure functions are attributive functions of the input parameters obtained in the QCD fit procedure at the scale Q_0^2 , then their uncertainty can be written applying the standard Hessian method

$$\Delta F = \left[\Delta\chi^2 \sum_{i,j=1}^k \frac{\partial F}{\partial p_i} C_{ij} \frac{\partial F}{\partial p_j} \right]^{\frac{1}{2}}. \quad (47)$$

Here we calculate the PPDFs uncertainty with $\Delta\chi^2 = 1$ which is the most appropriate choice in the polarized case. If one wishes to choose $\Delta\chi^2 > 1$, one simply can scale our error bands by $(\Delta\chi^2)^{1/2}$.

flavor	η	a	b	c	d
$u + \bar{u}$	0.783	0.409 ± 0.0025	2.733 ± 0.0368	0.0*	80.855 ± 1.4115
$d + \bar{d}$	-0.485	0.123 ± 0.0036	4.249 ± 0.0280	0.0*	83.345 ± 13.9609
\bar{u}	0.051 ± 0.0022	0.409 ± 0.0025	10.0*	10.016 ± 13.5510	-32.424 ± 15.8386
\bar{d}	-0.081 ± 0.0020	0.123 ± 0.0036	10.0*	116.235 ± 81.2783	902.567 ± 615.0900
\bar{s}	-0.072 ± 0.0077	0.123 ± 0.0036	10.0*	0.0*	-16.045 ± 4.7815
g	-0.156 ± 0.0039	2.453 ± 0.0334	10.0*	0.0*	-3.922 ± 0.0659

TABLE II: Final parameter values and their statistical errors at the input scale $Q_0^2 = 1 \text{ GeV}^2$, those parameters marked with (*) are fixed.

V. RESULTS

A. The quality of QCD fit

The values of obtained parameters attached to the input PPDFs are summarized in Table II. We find $\chi^2/\text{d.o.f.} = 1171.571/1132 = 1.03$ which yields an acceptable fit to the experimental data, the individual χ^2 for each set of data is presented in Table. I. The quality of the QCD fit to DIS and SIDIS asymmetry data is demonstrated in Fig. 3 and Fig. 4. Since we use many number of CLAS DIS data for proton and deuteron [20] and they do not situate in the Figure, we just show 8 of them for presentation. As can be seen the data are generally well described by the curves.

B. Extracted polarized parton distributions

In Fig. 5 we present the polarized parton distributions and their comparison to parameterizations from DSSV09 [55] and LSS10 [50] at input scale $Q_0^2 = 1 \text{ GeV}^2$.

Examining the $x(\delta u + \delta \bar{u})$ and $x(\delta d + \delta \bar{d})$ distributions we see that all of the fits are in agreement. For the $x\delta \bar{u}$ and $x\delta \bar{d}$ distributions, the curves, specially our model and DSSV09, are very close; $\delta \bar{d}$ is negative for any x in the measured x region while $\delta \bar{u}$ passes zero around $x = 0.1 - 0.2$ and becomes negative for large x for all presented models.

For the strange sea-quark density $x\delta s$, the main difference between the presented model, LSS10 and DSSV09 sets is that for $x < 0.03$ LSS10 is less negative than others, also both of current model and LSS10 are less positive than DSSV09 for $x > 0.03$. The other differences for the distributions comes from the fact that both DSSV09 and LSS10 analysis uses different number of data (we use the most and the newest ones) and DSSV09 uses pp collision data from RHIC which can impose individual constraints and effects on individual parton distributions in the nucleon [55]. As we mentioned, in the current analysis we focuss on the study of SIDIS data effect on determination of PPDFs, specially gluon and sea quarks separation which was not considered in our last DIS analysis. The impact of RHIC pp collision data will be considered in our near future analysis.

C. The impact of SIDIS data in determining the polarized sea-quark distributions

Generally speaking, polarized inclusive DIS data cannot distinguish \bar{u} , \bar{d} and \bar{s} but $\delta u = \delta d = \delta s = \delta \bar{s} = \delta \bar{q}$ is well determined and all the standard scenario NLO QCD analysis yield a negative value of it for any x in the measured region [24]. Employing SIDIS data a flavor decomposition of the polarized sea quarks is obtained and the light antiquark polarized densities $\delta \bar{u}$, $\delta \bar{d}$ and $\delta s = \bar{s}$ are determined separately, Fig. 6 shows the difference between $\delta \bar{u}$, $\delta \bar{d}$ in the current analysis comparing to other models and experimental data.

Also in the present parametrization we use a term $(1 + c_s x^{0.5} + d_s x)$ in the input strange sea-quark distribution to let a sign changing for $\delta s = \delta \bar{s}$, which was not considered in the standard scenario [22]. The comparison of polarized light sea-quark distributions ($x\delta s$, $x\delta \bar{u}$, $x\delta \bar{d}$) in the standard scenario and current model are presented in Fig. 7. It shows that the behavior of the polarized strange quark density remains puzzling [82].

Note that by having SIDIS data δs and $\delta \bar{s}$ can be separately determined as was done by the COMPASS collaboration recently [57]. However, it was demonstrated that there is no considerable difference between δs and $\delta \bar{s}$ in the x -range covered by their data. Also, the errors of the presented values of the difference $\delta s(x) - \delta \bar{s}(x)$ are quite large to allow us to conclude the assumption $\delta s(x) = \delta \bar{s}(x)$ like LSS10 and DSSV09. So, the above assumption and also the form of the fragmentation functions used to extract PPDFs by different groups may be possible causes of the contradiction between sea quarks densities obtained from the analyses of inclusive DIS data and combined inclusive and semi- inclusive DIS datasets [82].

D. The effect of COMPASS SIDIS data on polarized sea-quark distributions

As shown in Table I The measurement of SIDIS asymmetries for unidentified charged hadrons was performed by SMC collaboration and then the SIDIS asymmetries data for charged pion production from proton target and for charged kaon and pion production from a deuteron target was reported by HERMES. These asymmetries were used in the most DIS and SIDIS QCD analysis but

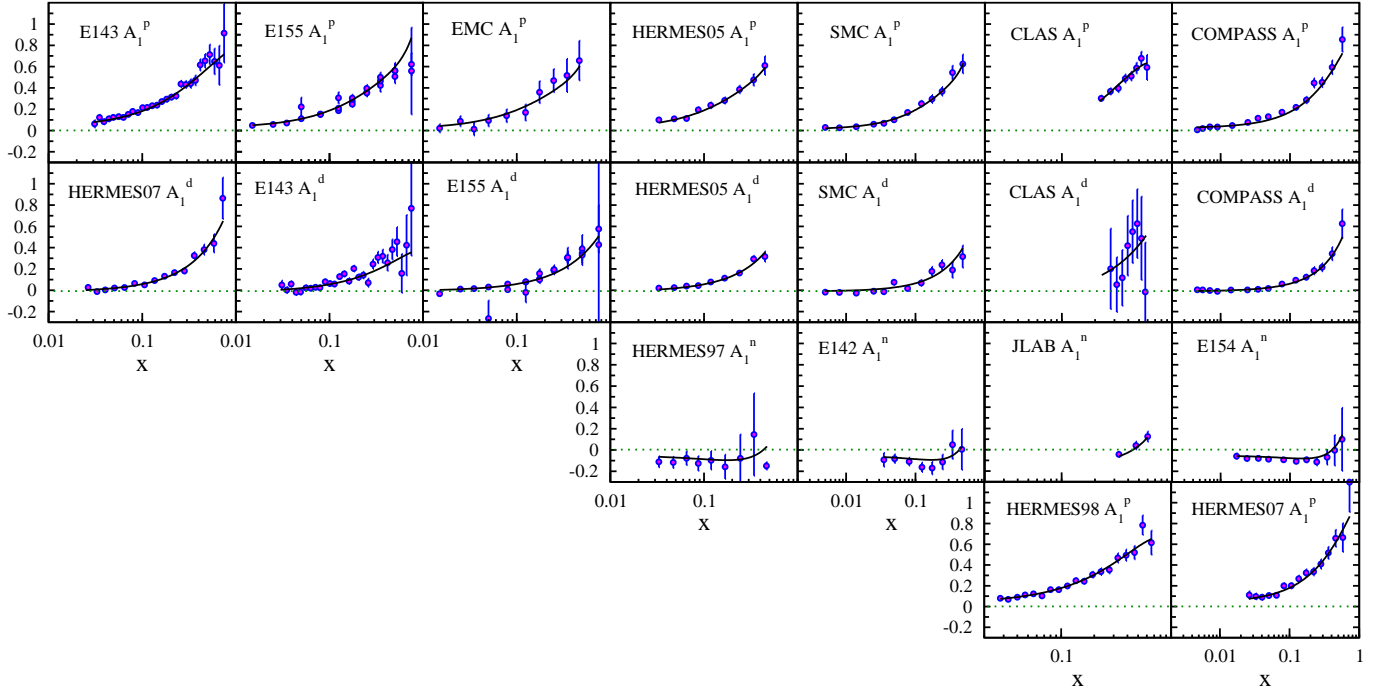


FIG. 3: Comparison of our NLO QCD results for the DIS asymmetries of proton, neutron and deuteron with the data at measured x and Q^2 .

the SIDIS asymmetry data from COMPASS are partially employed, specially the new semi inclusive asymmetries COMPASS data for scattering of muons from a polarized proton target for identified charged pions and kaons production; A_1^{p,π^\pm} and A_1^{p,k^\pm} [57], which was not available for the analysis before 2010.

In order to study the effect of COMPASS SIDIS data on polarized parton distributions, we show the comparison of our PPDFs results extracted from all datasets shown in Table I, and the PPDFs results extracted by excluding COMPASS SIDIS datasets in Fig. 8. As can be seen COMPASS data has effect on $\delta\bar{u}$, $\delta\bar{d}$ and $\delta s = \delta\bar{s}$ distributions since π^\pm and k^\pm are directly related to them. The changes of sea quark distributions are considerable in $0.07 \leq x \leq 0.4$ region that is well covered by the new COMPASS data. The distributions of $\delta u + \delta\bar{u}$, $\delta d + \delta\bar{d}$ and δg are not changed considerably.

E. Gluon polarization

In order to study the effect of SIDIS data on polarized gluon distribution, we perform another analysis with positive polarized gluon distribution. We understand that utilizing polarized DIS and SIDIS data in the QCD analysis can not enforce the positive or sign changing polarized gluon distributions and the data can not distinguish between these two scenarios, although the recent analyses

which employ both DIS and SIDIS data (and not pp collision data) could extract sign changing $x\delta g$ [50, 83]. In Table. III we present the values of obtained parameters in positive gluon scenario. We find $\chi^2/\text{d.o.f.} = 1.02$ which is almost equal to the one obtained from sign changing gluon scenario $\chi^2/\text{d.o.f.} = 1.03$. Fig. 9 shows the comparison of PPDFs extracted from positive and sign changing gluon scenarios. As can be seen all the distributions are almost not changed except $x\delta g$.

Fig. 10 shows the gluon distribution comparison between our previous standard scenario and the present sea flavor decomposition analysis. As presented, SU(2) and SU(3) symmetry breaking has direct effect on $x\delta g(x, Q^2)$ and makes it less. The gluon results of other models of both standard and light sea-quark decomposition scenario are also presented in Fig. 10 and they confirm this effect too [22, 24, 32, 50, 55].

We also calculated the ratio $\delta g/g$, using our extracted PPDFs for polarized gluon distributions and MRST02 [70] NLO QCD analysis for unpolarized gluon distributions. In Fig. 11 we present a comparison for $\delta g/g$ from LSS10, DSSV09 and our models (sign changing and positive gluon scenarios) at $Q^2 = 3 \text{ GeV}^2$ with measured value from experimental data [84–88]. Although we do not use the mentioned data in the current analysis, our results can predict the data very well.

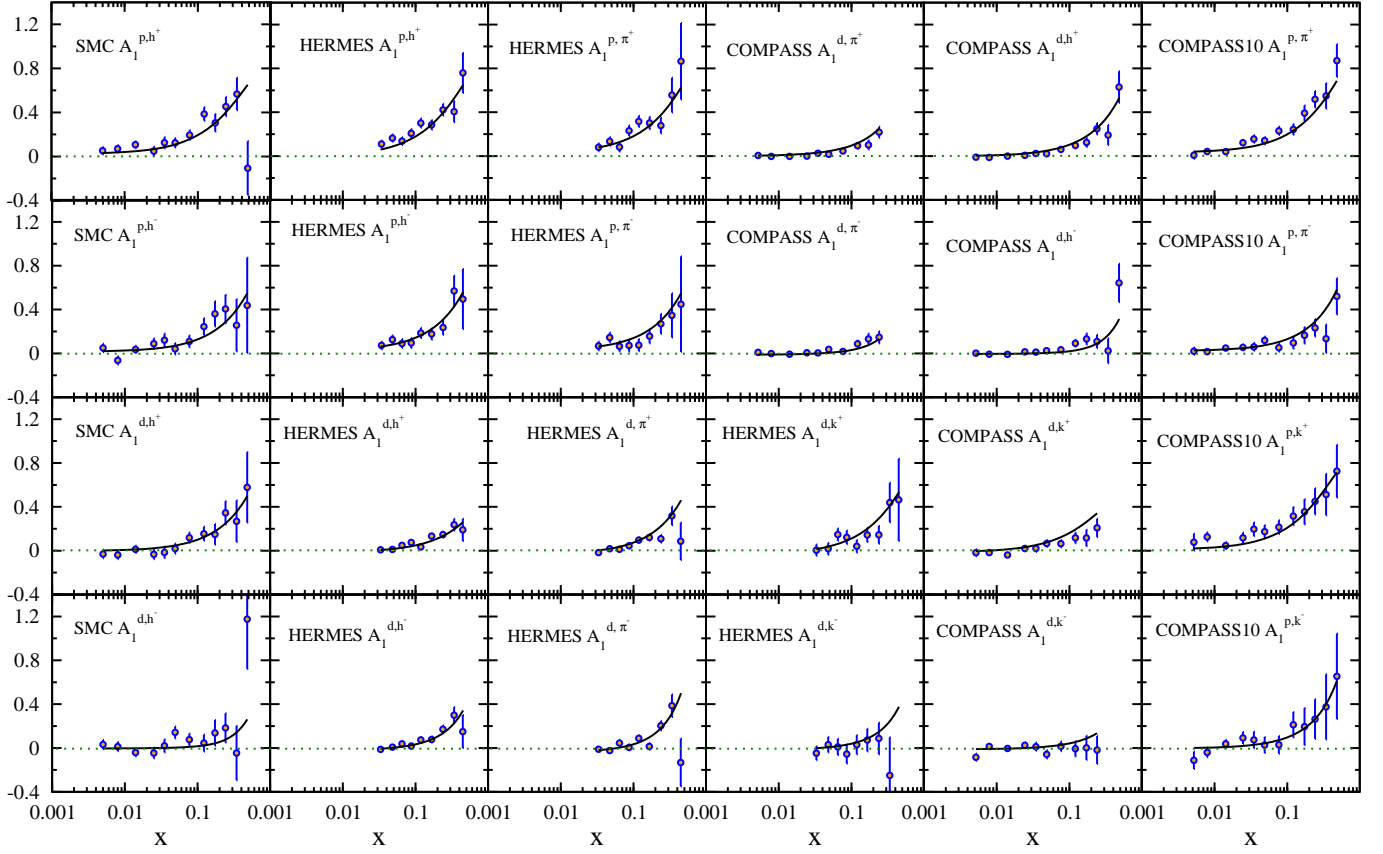


FIG. 4: Comparison of our NLO QCD results for the SIDIS asymmetries with the data at measured x and Q^2 .

flavor	η	a	b	c	d
$u + \bar{u}$	0.770	0.411 ± 0.0955	2.760 ± 0.1356	0.0*	78.145 ± 39.9149
$d + \bar{d}$	-0.498	0.125 ± 0.0080	4.221 ± 0.0359	0.0*	67.151 ± 4.0270
\bar{u}	0.051 ± 0.0004	0.411 ± 0.0955	10.0*	11.231 ± 0.4776	-32.425 ± 0.6351
\bar{d}	-0.081 ± 0.0003	0.125 ± 0.0080	10.0*	85.423 ± 2.4403	915.221 ± 26.7240
\bar{s}	-0.079 ± 0.0387	0.125 ± 0.0080	10.0*	0.0*	-15.843 ± 3.2887
g	0.081 ± 0.0008	3.958 ± 0.0326	10.0*	0.0*	25.820 ± 0.8029

TABLE III: Final parameter values and their statistical errors at the input scale $Q_0^2 = 1 \text{ GeV}^2$ for positive gluon scenario, those parameters marked with (*) are fixed.

F. Behavior of $\Delta\chi^2$

For more deliberation, in the preliminary QCD fit process we let all input parameters to vary. While investigating the behavior of $\Delta\chi^2$ we observe χ^2 increase consumedly in some points and a big amount of redundancy in parameters happens, this redundancy results into disorder of quadratic behavior of $\Delta\chi^2$. In order to have the Hessian method work as shown in Sec. IV B, we fix some parameters at their best obtained value so that Hessian matrix depends on the number of parameters which are independent sufficiently for the quadratic behavior of $\Delta\chi^2$, the detailed fixing and constraints in parameter space was discussed in Subsec. III B and Sec. IV.

To test of quadratic approximation in Eq. 39, Fig. 12 presents $\Delta\chi^2$ along some random samples of eigenvector directions and eigenvalues, $k = 1, 7, 9, 15$. The curves for middle values of $\lambda_{k=7,9}$ are very close to the ideal quadratic curve $\Delta\chi^2 = t^2$ and for other eigenvalues $\lambda_{k=1,15}$ we see some departure of ideal quadratic curve which shows the quadratic approximation is almost adequate, though imperfect. The behavior of the some odd curves, which are also available in other QCD analysis [80], usually correspond to the parameters controlling some unknown x -dependance parts of sea quarks and gluon densities.

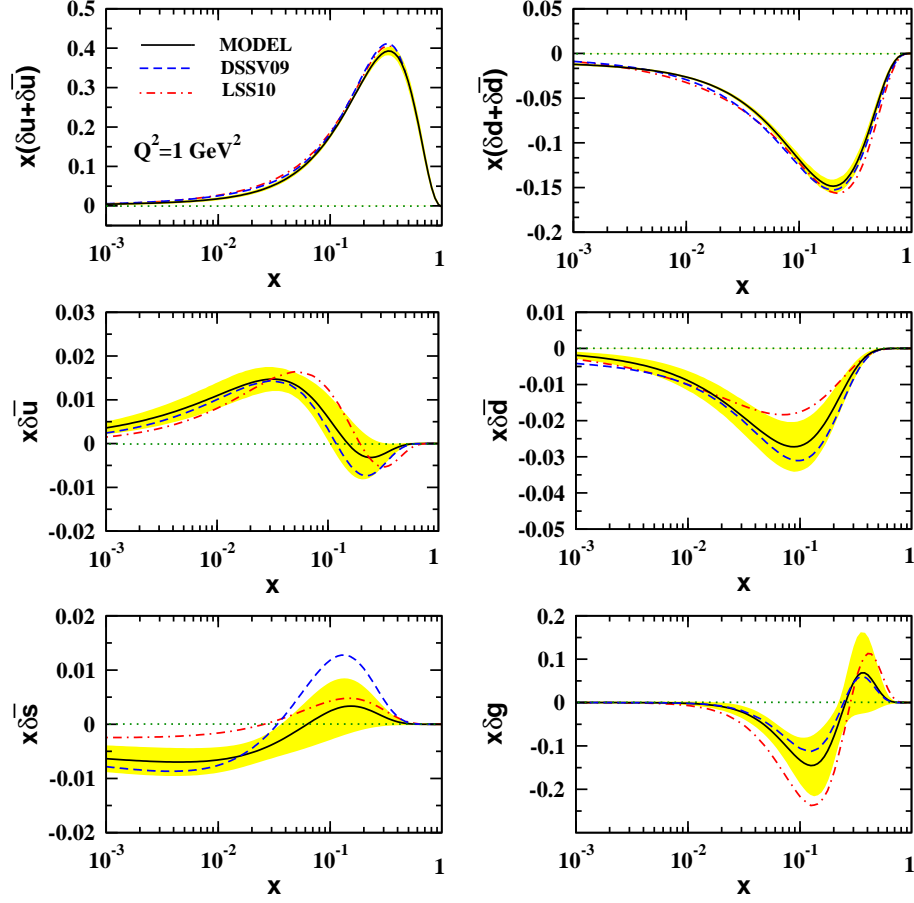


FIG. 5: The result of our analysis for quark helicity distributions at $Q_0^2 = 1 \text{ GeV}^2$ in comparison with DSSV09 [55] and LSS10 [50].

G. The spin sum rule

In the framework of QCD the spin $\frac{1}{2}$ of the proton can be defined in terms of the first moment of the total quark and gluon polarized densities and their orbital angular momentum

$$\frac{1}{2} = \frac{1}{2}\Delta\Sigma^p + \Delta g^p + L_z^p, \quad (48)$$

where L_z^p contains the total orbital angular momentum of all partons. The contribution of $\frac{1}{2}\Delta\Sigma + \Delta g$ in the scale of $Q^2 = 4 \text{ GeV}^2$ is around 0.010 in the present analysis. The reported values from DSSV09 [55] and LSS10 [50] are 0.026 and -0.212 respectively. For the positive gluon scenario LSS obtained 0.419 while our result is 0.367. In Table IV we compare the values of polarized PDFs first moment in NLO approximation with other recent analyses. Since the values of $\frac{1}{2}\Delta\Sigma$ are almost comparable, we observe and conclude that the difference between the reported values of $\frac{1}{2}\Delta\Sigma + \Delta g$ must be caused by different gluon distributions. Indeed, proliferation in PPDFs

data for sea quarks from SIDIS experiments eventuates to more accurate results for gluon distribution rather than analysis on DIS data merely, so one cannot yet come to a definite conclusion about the contribution of the orbital angular momentum to the total spin of the proton. The estimation of the valence spin distribution can be

Fit	$\Delta\bar{s}$	ΔG	$\Delta\Sigma$
DSSV09	-0.056	-0.096	0.245
LSS10	-0.063	0.316	0.207
LSS10 (δg pos)	-0.055	0.339	0.254
MODEL	-0.042	-0.138	0.256
MODEL (δg pos)	-0.046	0.245	0.244

TABLE IV: First moments of polarized PDFs at $Q^2 = 4 \text{ GeV}^2$. The corresponding DSSV09 and LSS10 values are also presented.

written as an accurate relation obtained from inclusive interactions in the experiments. Indeed one obtains the

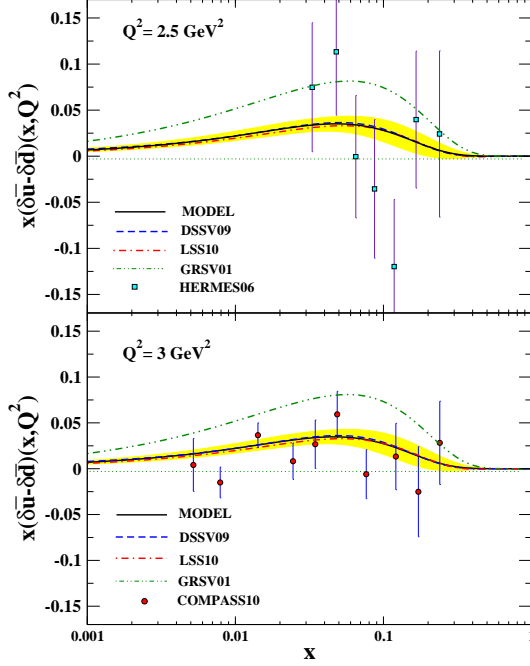


FIG. 6: The quark helicity distributions for the difference $x(\delta\bar{u} - \delta\bar{d})$ at $Q^2 = 2.5, 3 \text{ GeV}^2$ comparing to DSSV09 [55], LSS10 [50] and GRSV01 [32] and experimental data [16, 57].

following at LO [89]

$$\delta u_v + \delta d_v \sim \frac{36}{5} \frac{g_1^d}{(1 - 1.5\omega_D)}, \quad (49)$$

which is approximately true at NLO.

Theoretically, the first moment of the polarized valence distributions, truncated to the measured range of x ,

$$\Gamma_v(x_{\min} < x < x_{\max}) = \int_{x_{\min}}^{x_{\max}} [\delta u_v(x) + \delta d_v(x)] dx, \quad (50)$$

is obtained and shown for current model and DNS [53] in Table V. We obtain for the full measured range of x in SMC [47], HERMES [16] and COMPASS [89] experiments

$$\Gamma_v(0.003 < x < 0.7) = 0.454, \quad (51)$$

$$\Gamma_v(0.023 < x < 0.6) = 0.445, \quad (52)$$

$$\Gamma_v(0.006 < x < 0.7) = 0.459, \quad (53)$$

at $Q^2 = 10, 2.5$ and 10 GeV^2 respectively. Our value of Γ_v confirms the experimental results and the values come from DNS analysis.

An estimation of the sea quark first moment contribution to the nucleon spin can be generated by combining the values of Γ_v , Γ_1^N and a_8 [89]

$$\Delta\bar{u} + \Delta\bar{d} = 3\Gamma_1^N - \frac{1}{2}\Gamma_v + \frac{1}{12}a_8, \quad (54)$$

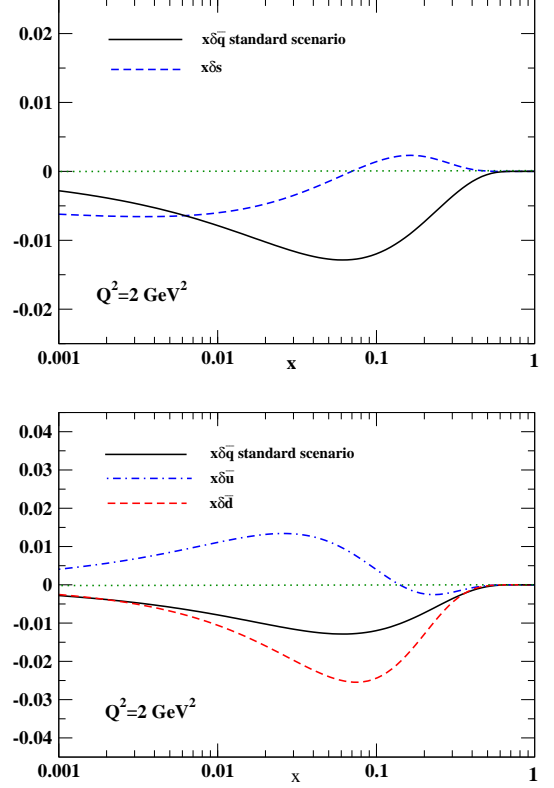


FIG. 7: The quark helicity distributions for $x\delta s$, $x\delta\bar{u}$ and $x\delta\bar{d}$ at $Q_0^2 = 2 \text{ GeV}^2$ comparing to $x\delta q$ obtained from the previous standard scenario [22].

where Γ_1^N is defined as the first moment of polarized structure function g_1 for the average nucleon N in an isoscalar target: $g_1^N = (g_1^p + g_1^n)/2$

$$\Gamma_1^N(Q^2 = 10 \text{ GeV}^2) = \int_0^1 g_1^N(x, Q^2) dx, \quad (55)$$

and ($a_8 = 3F - D$) evaluated from semi-leptonic hyperon decays. The result is reported to be zero for COMPASS experiment as shown in Table V. The zero value of $\Delta\bar{u} + \Delta\bar{d}$ suggests that $\Delta\bar{u}$ and $\Delta\bar{d}$, if they are not zero, must be in opposite sign. Previous estimation by SMC and HERMES are comparable with this supposition and are also given in Table V. The DNS parametrization, like the present model, finds a positive value for $\Delta\bar{u}$ and a negative value for $\Delta\bar{d}$, almost equal in absolute value. Opposite signs of $\Delta\bar{u}$ and $\Delta\bar{d}$ are anticipated in several models, e.g. in Ref. [32, 50, 55], see also [90] and references inside.

VI. SUMMARY

We have presented a NLO QCD analysis of the polarized DIS and SIDIS data on nucleon. During the analysis

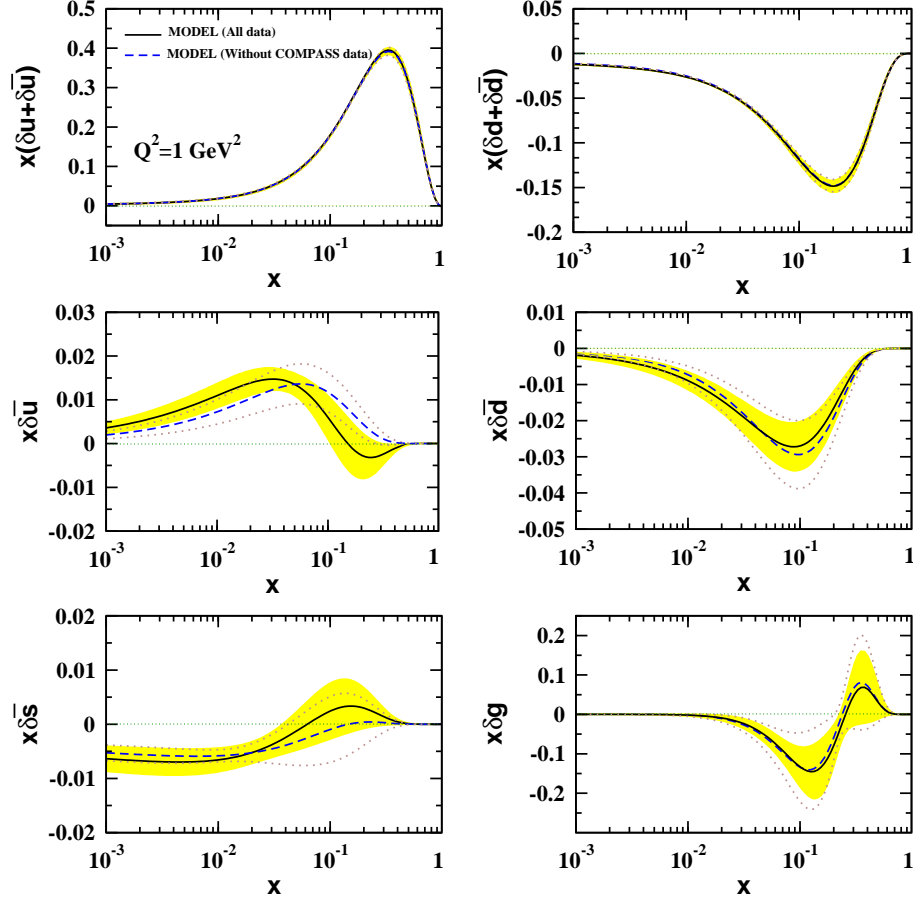


FIG. 8: The comparison of PPDFs results extracted from all datasets shown in Table I, and the PPDFs results extracted by excluding COMPASS SIDIS datasets at $Q_0^2 = 1 \text{ GeV}^2$. The corresponding error bands of them are also shown.

	x -range	Q^2 (GeV^2)	$\Delta u_v + \Delta d_v$			$\Delta \bar{u} + \Delta \bar{d}$		
			Exp.Value	DNS	MODEL	Exp.Value	DNS	MODEL
SMC98	0.003 – 0.7	10	$0.26 \pm 0.21 \pm 0.11$	0.386	0.454	$0.02 \pm 0.08 \pm 0.06$	-0.009	-0.043
HERMES05	0.023 – 0.6	2.5	$0.43 \pm 0.07 \pm 0.06$	0.363	0.445	$-0.06 \pm 0.04 \pm 0.03$	-0.005	-0.040
COMPASS07	0.006 – 0.7 0 – 1	10	$0.40 \pm 0.07 \pm 0.06$	0.385	0.459	–	-0.007	-0.043
			$0.41 \pm 0.07 \pm 0.06$	–	–	$0.0 \pm 0.04 \pm 0.03$	–	–

TABLE V: Evaluations of the first moments $\Delta u_v + \Delta d_v$ and $\Delta \bar{u} + \Delta \bar{d}$ from SMC [47], HERMES [16] and COMPASS [89] data and also from the DNS analysis [53] and present model truncated to the range of each relevant experiment. The SMC results were obtained with the assumption of a SU(3) symmetric sea: $\Delta \bar{u} = \Delta \bar{d} = \Delta \bar{s}$.

we consider SU(2) and SU(3) symmetry breaking scenario i.e. $\delta \bar{u} \neq \delta \bar{d} \neq \delta \bar{s}$, since the available experimental data are not enough to distinguish δs from $\delta \bar{s}$, we take them equal $\delta s = \delta \bar{s}$. The role of the semi-inclusive data in determining the polarized sea quarks is discussed and we have found also that the polarized gluon density is still ambiguous, this ambiguity is the main reason that the quark-gluon contribution into the total spin of the proton is still not well determined. We also calculate the error of PPDFs by standard Hessian method and investigate the quadratic behavior of $\Delta \chi^2$. Having extracted

the polarized PDFs, we compute the first moments of them and discuss about sum rules. In general, we find good agreement with the experimental data, and our results are in accord with other determinations specially DSSV09 and LSS10 which are the most precise ones. In conclusion, this demonstrates progress of the field toward a detailed description of the spin structure of the nucleon [83, 91–96]. The results of our new analysis applying pp collision data and studying the impact of fragmentation functions on PPDFs will be presented in a separate publication very soon.

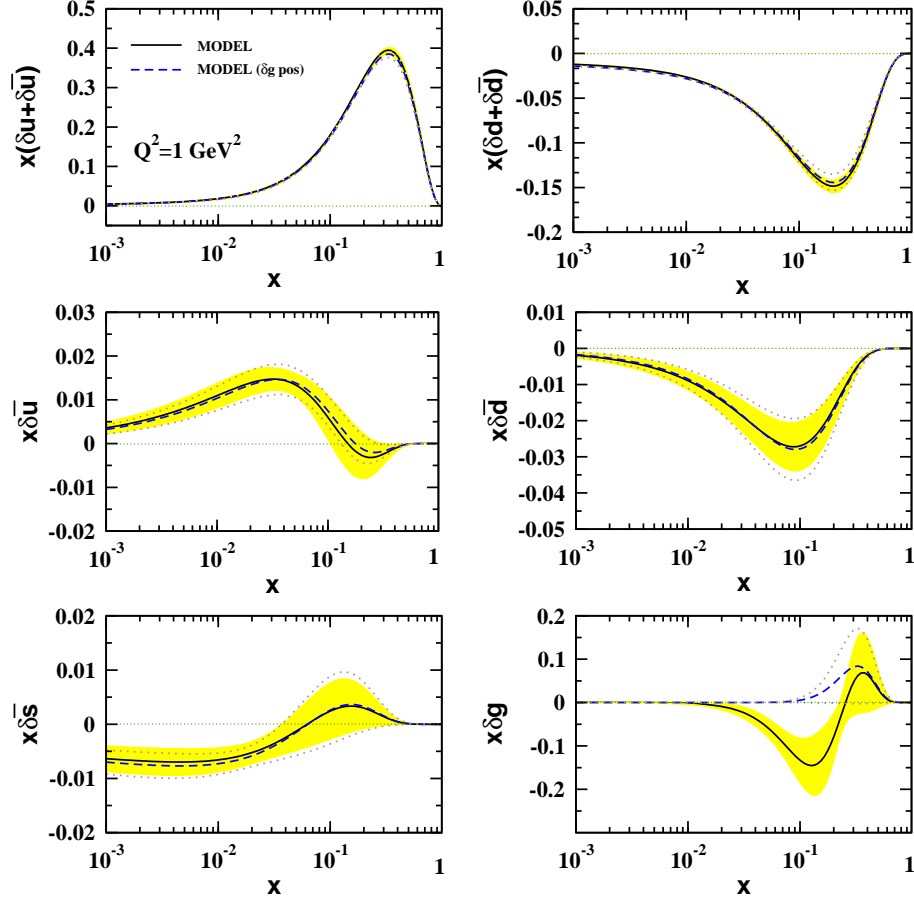


FIG. 9: The comparison of PPDFs results extracted from sign changing and positive gluon scenarios at $Q_0^2 = 1 \text{ GeV}^2$. The corresponding error bands of them are also shown.

VII. ACKNOWLEDGMENTS

We thank F. Olness for useful discussions and reading the manuscript. F.A appreciates M. Stratmann from DSSV for kind orientation and E. Kabuss from COM-PASS collaboration for communications. A.N.K thanks SITP (Stanford Institute for Theoretical Physics) for partial support and the Physics Department of SMU (Southern Methodist University) for their hospitality during the completion of this work. He is also grateful to CERN TH-PH division for the hospitality where a portion of this work was performed. This project was financially supported by Semnan University, Semnan University Science and Technology Park and the School of Particles and Accelerators, Institute for Research in Fundamental Sciences (IPM).

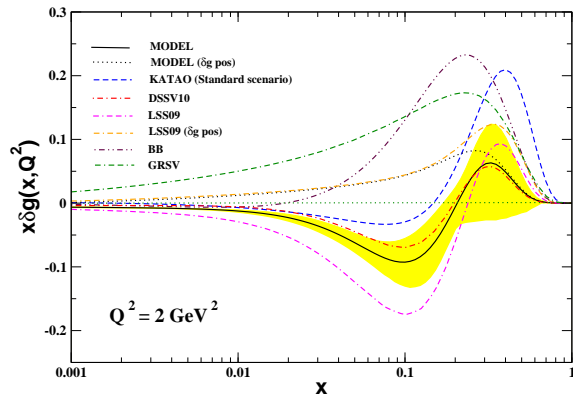


FIG. 10: The gluon helicity distributions at $Q^2 = 2 \text{ GeV}^2$ comparing to symmetry breaking [50, 55] and standard scenario [22, 24, 32] analysis.

Appendix A: Fortran code

A FORTRAN package containing our polarized parton distributions $x\delta u_v(x, Q^2)$, $x\delta d_v(x, Q^2)$,

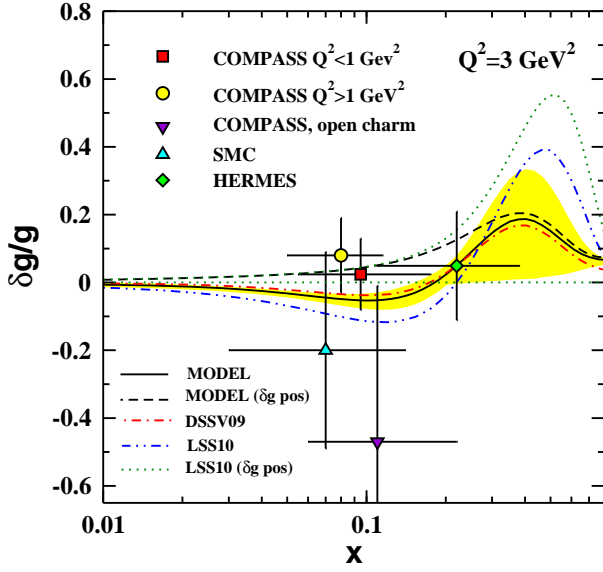


FIG. 11: The calculated ratio $\delta g/g$ for DSSV, LSS [50, 55] and our model in comparison with experimental data from

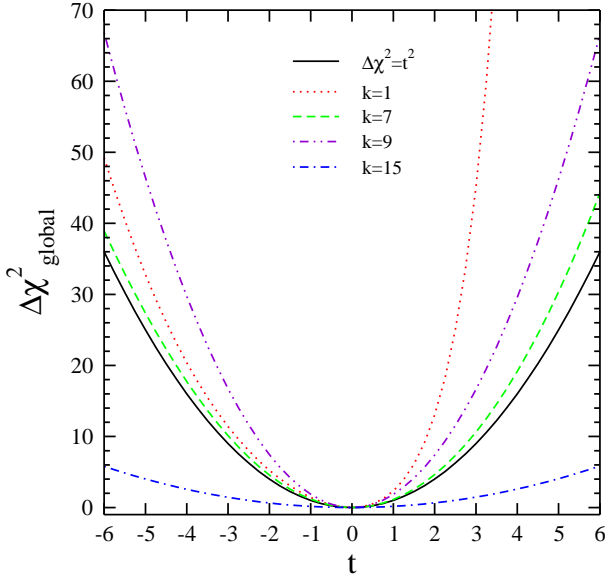


FIG. 12: $\Delta\chi^2_{\text{global}}$ as a function of t for some random sample eigenvectors.

$x\delta g(x, Q^2)$, $x\delta\bar{u}(x, Q^2)$, $x\delta\bar{d}(x, Q^2)$ and $x\delta s(x, Q^2)$ at NLO in the $\overline{\text{MS}}$ -scheme can be found in <http://particles.ipm.ir/links/QCD.htm> [97] or obtained via e-mail from the authors. These functions are interpolated using cubic splines in Q^2 and a linear interpolation in $\log(Q^2)$. The package includes an example program to illustrate the use of the routines.

Appendix B: N-moment of all polarized SIDIS Wilson coefficients

The transformation of Eq. 33 gives the SIDIS Wilson coefficients in $N - z$ space

$$C_{qq}(N, z) = C_f \left\{ -8\delta(1-z) + \tilde{P}_{qq}(z) \ln \frac{Q^2}{M^2} + L_1(z) + L_2(z) + (1-z) + \delta(1-z) \left[\left(\frac{1}{N} + \frac{1}{1+N} - 2\gamma - 2\Psi(N) - \frac{2}{N} - \frac{2}{N+1} + \frac{3}{2} \right) \ln \frac{Q^2}{M^2} + \frac{1}{6} \left(\frac{3}{N^2} + \frac{3}{(1+N)^2} + 6\gamma \left(\frac{1}{N} + \frac{1}{1+N} \right) + \pi^2 + 3\Psi(N) \times (4\gamma + \Psi(N)) + 3\Psi^2(N+2) - 6\frac{d\Psi(N)}{dN} \right) - \left(-\frac{1}{N^2} + \frac{1}{(1+N)^2} - 2\zeta(2, N+1) \right) + \frac{1}{N+N^2} \right] - 2(\gamma + \Psi(N)) \frac{1}{(1-z)_+} + (1+z)(\gamma + \Psi(N)) - \left(\frac{1}{N} + \frac{1}{1+N} \right) \frac{1}{(1-z)_+} + \frac{2(1+N+Nz)}{N+N^2} - \frac{2(1-z)}{N+N^2} \right\}, \quad (\text{B1})$$

$$C_{gq}(N, z) = C_f \left\{ \frac{1 + (1-z)^2}{z} \left[\ln \left(\frac{Q^2}{M^2} z(1-z) \right) - \gamma \right] - \Psi(N) + z + 2 \frac{1+2N-Nz}{N+N^2} - \frac{1+2N}{Nz+N^2z} - \frac{2z}{N+N^2} \right\}, \quad (\text{B2})$$

$$C_{qq}(N, z) = \frac{1}{2} \{ \delta(1-z) \times \left[-\frac{2-2N-(2+N+N^2)(\gamma + \Psi(N))}{N(1+N)(2+N)} + \frac{2}{2+3N+N^2} \right] + \frac{2+N+N^2}{2N+3N^2+N^3} \left[\frac{1}{(1-z)_+} + \frac{1}{z} - 2 \right] \}, \quad (\text{B3})$$

$$\delta C_{qq}(N, z) = C_{qq}^1 - 2C_f \frac{1}{N + N^2} (1 - z), \quad (\text{B4})$$

$$\delta C_{qq}(N, z) = C_{qq}^1 - 2C_f \frac{1}{N + N^2} z, \quad (\text{B5})$$

$$\begin{aligned} \delta C_{qg}(N, z) = & \frac{1}{2} \left\{ \delta(1 - z) \left[-\frac{2 + (N - 1)(\gamma + \Psi(N))}{N(1 + N)} \right. \right. \\ & \left. \left. + \frac{2}{N + N^2} \right] \right. \\ & \left. + \frac{N - 1}{N(1 + N)} \left[\frac{1}{(1 - z)_+} + \frac{1}{z} - 2 \right] \right\}, \quad (\text{B6}) \end{aligned}$$

where $C_f = 4/3$, $\gamma \simeq 0.577216$ and

$$\tilde{P}_{qq}(z) = \frac{1 + z^2}{(1 - z)_+} + \frac{3}{2} \delta(1 - z), \quad (\text{B7})$$

$$L_1(z) = (1 + z^2) \left(\frac{\ln(1 - z)}{1 - z} \right), \quad (\text{B8})$$

$$L_2(z) = \frac{1 + z^2}{1 - z} \ln z, \quad (\text{B9})$$

$$\int_0^1 dz f(z)(g(z))_+ \equiv \int_0^1 dz [f(z) - f(1)]g(z) \quad (\text{B10})$$

-
- [1] J. Ashman *et al.* [European Muon Collaboration], Phys. Lett. B **206** (1988) 364.
- [2] J. Ashman *et al.* [European Muon Collaboration], Nucl. Phys. B **328** (1989) 1.
- [3] G. Altarelli, arXiv:0907.1751 [hep-ph].
- [4] M. Anselmino, A. Efremov and E. Leader, Phys. Rept. **261** (1995) 1 [Erratum-ibid. **281** (1997) 399] [arXiv:hep-ph/9501369].
- [5] E. W. Hughes and R. Voss, Ann. Rev. Nucl. Part. Sci. **49** (1999) 303.
- [6] B. Lampe and E. Reya, Phys. Rept. **332** (2000) 1 [arXiv:hep-ph/9810270].
- [7] B. W. Filippone and X. D. Ji, Adv. Nucl. Phys. **26** (2001) 1 [arXiv:hep-ph/0101224].
- [8] J. Ashman *et al.* [European Muon Collaboration], Phys. Lett. B **206** (1988) 364; J. Ashman *et al.* [European Muon Collaboration], Nucl. Phys. B **328** (1989) 1.
- [9] B. Adeva *et al.* [Spin Muon Collaboration], Phys. Rev. D **58** (1998) 112001.
- [10] M. G. Alekseev *et al.* [COMPASS Collaboration], Phys. Lett. B **690**, 466 (2010) [arXiv:1001.4654 [hep-ex]], V. Y. Alexakhin *et al.* [COMPASS Collaboration], Phys. Lett. B **647** (2007) 8 [arXiv:hep-ex/0609038].
- [11] P. L. Anthony *et al.* [E142 Collaboration], Phys. Rev. D **54** (1996) 6620 [arXiv:hep-ex/9610007].
- [12] K. Abe *et al.* [E143 collaboration], Phys. Rev. D **58** (1998) 112003 [arXiv:hep-ph/9802357].
- [13] K. Abe *et al.* [E154 Collaboration], Phys. Rev. Lett. **79** (1997) 26 [arXiv:hep-ex/9705012].
- [14] P. L. Anthony *et al.* [E155 Collaboration], Phys. Lett. B **493** (2000) 19 [arXiv:hep-ph/0007248].
- [15] P. L. Anthony *et al.* [E155 Collaboration], Phys. Lett. B **463** (1999) 339 [arXiv:hep-ex/9904002].
- [16] A. Airapetian *et al.* [HERMES Collaboration], Phys. Rev. D **71** (2005) 012003 [arXiv:hep-ex/0407032].
- [17] K. Ackerstaff *et al.* [HERMES Collaboration], Phys. Lett. B **404** (1997) 383 [arXiv:hep-ex/9703005], A. Airapetian *et al.* [HERMES Collaboration], Phys. Lett. B **442** (1998) 484 [arXiv:hep-ex/9807015].
- [18] A. Airapetian *et al.* [HERMES Collaboration], Phys. Rev. D **75** (2007) 012007 [arXiv:hep-ex/0609039].
- [19] X. Zheng *et al.* (JLab/Hall A Collaboration), Phys. Rev. Lett. **92**, 012004 (2004); Phys. Rev. C **70**, 065207 (2004).
- [20] K. V. Dharmawardane *et al.* [CLAS Collaboration], Phys. Lett. B **641** (2006) 11 [arXiv:nucl-ex/0605028].
- [21] R. D. Ball *et al.* [The NNPDF Collaboration], Nucl. Phys. B **874**, 36 (2013) [arXiv:1303.7236 [hep-ph]].
- [22] A. N. Khorramian, S. Atashbar Tehrani, S. Taheri Monfared, F. Arbabifar and F. I. Olness, Phys. Rev. D **83** (2011) 054017 [arXiv:1011.4873 [hep-ph]].
- [23] T. Gehrmann and W. J. Stirling, Phys. Rev. D **53** (1996) 6100, hep-ph/9512406.
- [24] J. Blumlein and H. Bottcher, Nucl. Phys. B **841** (2010) 205 [arXiv:1005.3113 [hep-ph]].
- [25] G. Altarelli, R. D. Ball, S. Forte and G. Ridolfi, Acta Phys. Polon. B **29** (1998) 1145 [arXiv:hep-ph/9803237].
- [26] R. D. Ball, G. Ridolfi, G. Altarelli and S. Forte, arXiv:hep-ph/9707276.
- [27] C. Bourrely, F. Buccella, O. Pisanti, P. Santorelli and J. Soffer, Prog. Theor. Phys. **99** (1998) 1017 [arXiv:hep-ph/9803229].
- [28] L. E. Gordon, M. Goshtasbpour and G. P. Ramsey, Phys. Rev. D **58** (1998) 094017 [arXiv:hep-ph/9803351].
- [29] E. Leader, A. V. Sidorov and D. B. Stamenov, Phys. Lett. B **462** (1999) 189 [arXiv:hep-ph/9905512]; E. Leader, A. V. Sidorov and D. B. Stamenov, Phys. Lett. B

- 445** (1998) 232 [arXiv:hep-ph/9808248], E. Leader, A. V. Sidorov and D. B. Stamenov, Phys. Rev. D **58** (1998) 114028 [arXiv:hep-ph/9807251]; E. Leader, A. V. Sidorov and D. B. Stamenov, Int. J. Mod. Phys. A **13** (1998) 5573 [arXiv:hep-ph/9708335].
- [30] M. Stratmann, Nucl. Phys. Proc. Suppl. **79** (1999) 538 [arXiv:hep-ph/9907465].
- [31] D. K. Ghosh, S. Gupta and D. Indumathi, Phys. Rev. D **62** (2000) 094012 [arXiv:hep-ph/0001287].
- [32] M. Gluck, E. Reya, M. Stratmann and W. Vogelsang, Phys. Rev. D **63**, 094005 (2001) [arXiv:hep-ph/0011215].
- [33] R. S. Bhalerao, Phys. Rev. C **63** (2001) 025208 [arXiv:hep-ph/0003075].
- [34] E. Leader, A. V. Sidorov and D. B. Stamenov, Eur. Phys. J. C **23** (2002) 479 [arXiv:hep-ph/0111267].
- [35] J. Blumlein and H. Bottcher, Nucl. Phys. B **636** (2002) 225 [arXiv:hep-ph/0203155].
- [36] Y. Goto *et al.* [Asymmetry Analysis collaboration], Phys. Rev. D **62** (2000) 034017 [arXiv:hep-ph/0001046]; M. Hirai, S. Kumano and N. Saito [Asymmetry Analysis Collaboration], Phys. Rev. D **69** (2004) 054021 [arXiv:hep-ph/0312112].
- [37] E. Leader, A. V. Sidorov and D. B. Stamenov, Phys. Rev. D **73** (2006) 034023 [arXiv:hep-ph/0512114].
- [38] C. Bourrely, J. Soffer and F. Buccella, “A statistical approach for polarized parton distributions,” Eur. Phys. J. C **23** (2002) 487 [arXiv:hep-ph/0109160].
- [39] G. Altarelli *et al.*, Nucl. Phys. **B496** (1997) 337; Acta Phys. Pol. **B29** (1998) 1145; S. Forte, M. Mangano, and G. Ridolfi, Nucl. Phys. **B602** (2001) 585.
- [40] G. Altarelli, R. D. Ball, S. Forte and G. Ridolfi, “Determination of the Bjorken sum and strong coupling from polarized structure functions,” Nucl. Phys. B **496** (1997) 337 [arXiv:hep-ph/9701289].
- [41] M. Hirai and S. Kumano [Asymmetry Analysis Collaboration], Nucl. Phys. B **813**, 106 (2009) [arXiv:0808.0413 [hep-ph]].
- [42] A. N. Khorramian, A. Mirjalili and S. A. Tehrani, JHEP **0410** (2004) 062 [arXiv:hep-ph/0411390].
- [43] S. Atashbar Tehrani and A. N. Khorramian, JHEP **0707**, 048 (2007) [arXiv:0705.2647 [hep-ph]].
- [44] S. Atashbar Tehrani, A. N. Khorramian, S. Taheri Monfared and F. Arbabifar, AIP Conf. Proc. **1374**, 391 (2011).
- [45] F. Arbabifar, A. N. Khorramian, S. Taheri Monfared and S. Atashbar Tehrani, Int. J. Mod. Phys. A **26**, 625 (2011).
- [46] A. N. Khorramian, S. Atashbar Tehrani, F. Olness, S. Taheri Monfared and F. Arbabifar, Nucl. Phys. Proc. Suppl. **207-208**, 65 (2010).
- [47] SMC Collaboration, B. Adeva *et al.*, Phys. Lett. B **420** (1998) 180.
- [48] M.G. Alekseev *et al.* (COMPASS Collaboration), Phys. Lett. B **660**, 458 (2008).
- [49] M.G. Alekseev *et al.* (COMPASS Collaboration), Phys. Lett. B **680**, 217 (2009).
- [50] E. Leader, A. V. Sidorov and D. B. Stamenov, Phys. Rev. D **82** (2010) 114018 [arXiv:1010.0574 [hep-ph]].
- [51] D. de Florian, O. A. Sampayo, and R. Sassot, Phys. Rev. D **57**, 5803 (1998); D. de Florian and R. Sassot, Phys. Rev. D **62**, 094025 (2000); D. de Florian, G. A. Navarro, and R. Sassot, Phys. Rev. D **71**, 094018 (2005).
- [52] D. de Florian and R. Sassot, Phys. Rev. D **62** (2000) 094025 [arXiv:hep-ph/0007068].
- [53] D. de Florian, G. A. Navarro and R. Sassot, Phys. Rev. D **71** (2005) 094018 [arXiv:hep-ph/0504155].
- [54] D. de Florian, R. Sassot, M. Stratmann and W. Vogelsang, Phys. Rev. Lett. **101**, 072001 (2008) [arXiv:0804.0422 [hep-ph]].
- [55] D. de Florian, R. Sassot, M. Stratmann and W. Vogelsang, Phys. Rev. D **80** (2009) 034030 [arXiv:0904.3821 [hep-ph]].
- [56] M. Soleymaninia, A. N. Khorramian, S. M. Moosavinejad and F. Arbabifar, Phys. Rev. D **88**, 054019 (2013) [arXiv:1306.1612 [hep-ph]].
- [57] M. G. Alekseev *et al.* [COMPASS Collaboration], Phys. Lett. B **693** (2010) 227 [arXiv:1007.4061 [hep-ex]].
- [58] M. Arneodo *et al.* (NMC Collaboration), Phys. Lett. B **364**, 107 (1995).
- [59] K. Abe *et al.* (SLAC E143 Collaboration), Phys. Lett. B **452**, 194 (1999).
- [60] S. D. Bass, Rev. Mod. Phys. **77**, 1257 (2005) [hep-ph/0411005].
- [61] D. Adams *et al.*, SMC Collaboration, Phys. Lett. B **336** (1994) 125.
- [62] K. Abe *et al.*, E154 Collaboration, Phys. Lett. B **404** (1997) 377.
- [63] S. Wandzura, F. Wilczek, Phys. Lett. B **72** (1977) 195.
- [64] D. de Florian, M. Stratmann, and W. Vogelsang, Phys. Rev. D **57**, 5811 (1998).
- [65] A. N. Sisakian, O. Y. Shevchenko and V. N. Samoilov, hep-ph/0010298.
- [66] E. Leader, A. V. Sidorov and D. B. Stamenov, arXiv:1212.3204.
- [67] M. Hirai, S. Kumano, T. -H. Nagai and K. Sudoh, Phys. Rev. D **75**, 094009 (2007) [hep-ph/0702250].
- [68] S. Albino, B. A. Kniehl and G. Kramer, Nucl. Phys. B **803**, 42 (2008) [arXiv:0803.2768 [hep-ph]].
- [69] D. de Florian, R. Sassot, and M. Stratmann, Phys. Rev. D **75**, 114010 (2007); Phys. Rev. D **76**, 074033 (2007).
- [70] A. D. Martin, R. G. Roberts, W. J. Stirling and R. S. Thorne, Eur. Phys. J. C **28**, 455 (2003) [hep-ph/0211080].
- [71] J. Soffer, Phys. Rev. Lett. **74**, 1292 (1995) [hep-ph/9409254].
- [72] C. Amsler *et al.* (Particle Data Group), Phys. Lett. B **667** (2008) 1.
- [73] H. J. Lipkin, Phys. Lett. B **214**, 429 (1988); Phys. Lett. B **230**, 135 (1989); F. E. Close and R. G. Roberts, Phys. Rev. Lett. **60**, 1471 (1988); M. Roos, Phys. Lett. B **246**, 179 (1990); Z. Dziembowski and J. Franklin, J. Phys. G **17**, 213 (1991). P. G. Ratcliffe, Phys. Lett. B **242**, 271 (1990); Phys. Lett. B **365**, 383 (1996); arXiv:hep-ph/0012133; S. L. Zhu, G. Sacco, and M. J. Ramsey-Musolf, Phys. Rev. D **66**, 034021 (2002); E. Leader and D. B. Stamenov, Phys. Rev. D **67**, 037503 (2003).
- [74] M. A. Ahmed and G. G. Ross, Nucl. Phys. B **111**, 441 (1976); G. Altarelli and G. Parisi, Nucl. Phys. B **126**, 298 (1977).
- [75] R. Mertig and W. L. van Neerven, Z. Phys. C **70**, 637 (1996); W. Vogelsang, Phys. Rev. D **54**, 2023 (1996); Nucl. Phys. B **475**, 47 (1996).
- [76] M. Stratmann and W. Vogelsang, Phys. Rev. D **64**, 114007 (2001).
- [77] G. Altarelli, R. K. Ellis, G. Martinelli and S. Y. Pi, Nucl. Phys. B **160**, 301 (1979).
- [78] A. Vogt, Comput. Phys. Commun. **170**, 65 (2005)

- [arXiv:hep-ph/0408244].
- [79] F. James, MINUIT, CERN Program Library Long Writeup **D506**.
 - [80] A. D. Martin, W. J. Stirling, R. S. Thorne and G. Watt, Eur. Phys. J. C **63**, 189 (2009) [arXiv:0901.0002 [hep-ph]].
 - [81] J. Pumplin, D. Stump, R. Brock, D. Casey, J. Huston, J. Kalk, H. L. Lai and W. K. Tung, Phys. Rev. D **65**, 014013 (2001) [hep-ph/0101032].
 - [82] E. Leader, A. V. Sidorov and D. B. Stamenov, Phys. Rev. D **84**, 014002 (2011) [arXiv:1103.5979 [hep-ph]].
 - [83] A. Sissakian, O. Shevchenko and O. Ivanov, Eur. Phys. J. C **65**, 413 (2010) [arXiv:0908.3296 [hep-ph]].
 - [84] A. Airapetian *et al.* [HERMES Collaboration], Phys. Rev. Lett. **84**, 2584 (2000) [hep-ex/9907020].
 - [85] B. Adeva *et al.* [Spin Muon (SMC) Collaboration], Phys. Rev. D **70**, 012002 (2004) [hep-ex/0402010].
 - [86] M. Stolarski [COMPASS Collaboration], arXiv:0809.1803 [hep-ex].
 - [87] E. S. Ageev *et al.* [COMPASS Collaboration], Phys. Lett. B **633**, 25 (2006) [hep-ex/0511028].
 - [88] M. Alekseev *et al.* [COMPASS Collaboration], arXiv:0802.3023 [hep-ex].
 - [89] M. Alekseev *et al.* [COMPASS Collaboration], Phys. Lett. B **660**, 458 (2008) [arXiv:0707.4077 [hep-ex]].
 - [90] J.C. Peng, Eur. Phys. J. A **18** (2003) 395.
 - [91] J. Soffer, arXiv:1112.0304 [hep-ph].
 - [92] O. Y. Shevchenko, R. R. Akhunzyanov and V. Y. Lavrentyev, Eur. Phys. J. C **71**, 1713 (2011) [arXiv:1106.4795 [hep-ph]].
 - [93] E. Leader, A. V. Sidorov and D. B. Stamenov, arXiv:1012.5033 [hep-ph].
 - [94] D. de Florian and W. Vogelsang, Phys. Rev. D **81**, 094020 (2010) [arXiv:1003.4533 [hep-ph]].
 - [95] D. Boer *et al.*, arXiv:1108.1713 [nucl-th].
 - [96] D. de Florian and Y. R. Habarnau, Eur. Phys. J. C **73**, 2356 (2013) [Eur. Phys. J. C **73**, 2356 (2013)] [arXiv:1210.7203 [hep-ph]].
 - [97] Program summary: <http://particles.ipm.ir/links/QCD.htm>.